A New Measure of Wind Power Variability with Implications for the Optimal Sizing of Standalone Wind Power Systems

Abstract
This paper proposes a new measure of wind power variability and investigates the impacts of wind power variability on the optimal sizing of SWP systems. The proposed new measure of the wind power variability in the frequency domain, which mainly includes a cumulative energy distribution index and a fluctuation factor, is applied to assess the variability of wind power throughout 6 consecutive years from 6 far apart sites from latitude 0° to 50° across America. Big data assessment results indicate the intermittent wind power at one site can be treated as Quasi-Time-Invariant (QTI) in the frequency domain. Big data simulations of the six SWP systems with the same residential load demand at the six sites provide QTI responses of the power supply reliability against the sizing of the system components in the mitigation of wind power variability. A case study of the optimal sizing of a SWP system at Chicago, was carried out, which aims is to minimize the system cost while satisfying the requirement of power supply reliability. It can be found from the study that, the proposed approach provides a new way to significantly reduce the computation in the optimal sizing of SWP systems.

***Keywords*:**
Wind power variability measurement; Standalone wind power system; Power fluctuation mitigation; Power supply reliability; Optimal sizing

1. Introduction

Standalone Wind Power (SWP) systems which mainly or completely rely on the electricity generated from intermittent wind power, are widely used in remote areas where mains electricity and/or conventional fuels are unavailable or cost-prohibitive [1-4]. Power supply reliability and cost-effectiveness are two primary concerns of most SWP system owners [5-8]. A typical SWP system generally consists of a wind turbine, a battery bank, and loads. Optimal sizing is a crucial step in the development of SWP systems with dominant or full wind energy penetration, which mainly involves how to determine the proper sizes of the wind turbine and the battery bank. The size of the wind turbine, which is based on the average wind speed across many years, is usually devised to allow the wind power plant to produce sufficient power to meet the load demand [1]. However, the mismatch between intermittent wind power and varying load demand, especially the intermittent wind power, would cause power outages in the case of deficit wind power supply and power losses in the case of excessive wind power supply. To increase the power supply reliability and the system efficiency, the battery energy storage is incorporated to make the wind power dispatchable while incurring a possible significant initial cost of battery [9-15]. Oversized wind turbine also helps reduce the power outages at the expense of an extra installed cost of the wind turbine [16]. In addition, standby diesel generators can be optionally added into SWP systems to compensate power outages, but would incur expensive costs of carbon-emitting fuel, operation and maintenance in the life cycle [17-19]. Apparently, wind power variability/fluctuation has significant techno-economic impacts on the deployment of SWP systems [20, 21].

Hence the optimal sizing is a key factor to allow SWP systems to supply a reliable power at a low cost. It is critical to better understand the characteristics of wind power variability in order to develop more reliable, efficient and cost-effective wind power systems. Thus far, in the time domain, the wind speed variations at different time scales [22], the step change analysis of the power produced by a wind plant or summed plants [23] and the duty ratio of wind speed ramp [24, 25] are used to evaluate the wind power variability, which are used to define the dynamics of fill-in power from energy storage and generation for mitigating wind power fluctuations in the case of large-scale grid-connected wind plants. The power spectrum analyses in the frequency domain are proposed to characterize the variability of the power output from a wind plant or summed plants – the Power Spectra Density (PSD) of the measured power output of an individual wind turbine is found to follow a Kolmogorov spectrum at high frequency, while the PSD of interconnected wind plants follows a smoothing spectrum with a rapid decrease at high frequency [22, 23, 26-28]. All aforementioned measurements of wind power intermittency in both the time domain and the frequency domain show that the interconnection of wind plants could bring a significant reduction of high-frequency wind power variability which indicate wind power variability can be mitigated by slow-ramping energy storage or power generation. Hence the impacts of wind power variability should be taken into consideration in the development of SWP systems. Unlike interconnected wind power systems, the battery bank is defaulted as effective energy

storage device for wind power variability mitigation in practice. For SWP systems, many optimization algorithms have been attempted to globally search the optimal sizes of system components, e.g. iterative algorithms, generic algorithms etc. [29]-[35]. However, it is vague that how the optimal sizing of these standalone systems can be efficiently achieved by using these optimization techniques without taking the impacts of wind power variability into careful consideration. Given full or high penetration of random and uncontrollable wind power in SWP systems, it remains an open issue to quantify the wind power variability and the impacts of wind power variability on the optimal sizing of SWP systems, especially on the determination of battery capacity [13, 29].

In spite of the stochastic intermittence, both wind power and load demand are quasi-periodic at different timescale [30]. For instance, the peaks and valleys of wind power production or load consumption vary with seasons. Thus, in this paper, both annual wind power generation and generation-load mismatch power are approximately represented as a combination of sinusoidal power harmonics and DC power component with inter-annual variations. Accordingly, the power fluctuations of SWP systems can be considered as a power harmonics source. Subsequently, a power spectrum based energy distribution index and a total harmonic distortion based fluctuation factor are developed to evaluate the wind power variability in the frequency domain. Big data analysis of wind power of six far apart sites across America during 2007-2012 illustrated that, in terms of the proposed energy distribution index and fluctuation factor, the intermittent wind power can be treated as Quasi-Time-Invariant (QTI) in the frequency domain. Consequently, both the low-pass energy filtering capability of the battery and the power gap filling capability of the wind generator are investigated. Big data simulations of the SWP system with the same residential load demand at the six sites as carried out to provide QTI datasheets of the power supply reliability against the battery capacity and the wind turbine size for simplifying the optimal sizing of SWP systems. A case study is given to demonstrate how to take the impacts of wind power variability into consideration for the optimal sizing of SWP systems.

2. Standalone Wind Power System

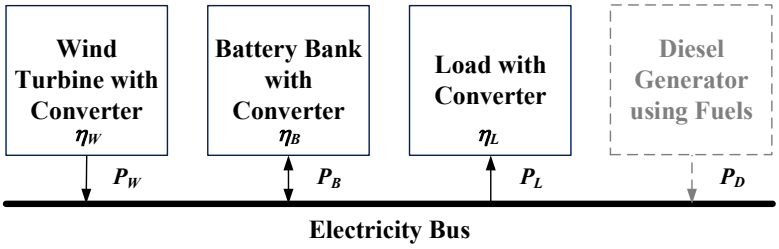

Fig. 1. A typical SWP system with/without diesel generator

The diagram of a typical SWP system is illustrated in Fig. 1. The SWP system consists of a wind generator, an energy storage battery bank and a residential load, where power converters act as the power interfaces of the wind generator/battery/load to the electricity bus [22] with the wind turbine conversion efficiency $\eta_W \le 95\%$, the load conversion efficiency $\eta_L \le 95\%$ and the battery round-trip efficiency $\eta_B \le 81\%$ [23, 24]. The dispatchable standby diesel generator might be optionally installed to improve the power supply reliability and reduce the required battery capacity. However, the hybrid wind-diesel standalone systems will lead to expensive fuel consumption, operation and maintenance costs and carbon emission in addition to the installation cost. The hybrid system would not be investigated hereinafter.

2.1. Operation Scenarios

The operation of SWP system includes four scenarios:

- When $P_W \ge P_L$ and the battery is not overcharged, the load demand P_L is met and the battery bank is charged with the excessive power $\Delta P = P_W - P_L \ge 0$.
- When $P_W \ge P_L$ and the battery is fully charged, the load demand P_L is met and the excessive power $\Delta P = P_W - P_L \ge 0$ is discarded as power loss.
- When $P_W < P_L$ and the battery is not over-discharged, the battery bank releases power to compensate the power deficit $\Delta P = P_W - P_L \le 0$.
- When $P_W < P_L$ and the battery is over-discharged, the battery bank is charged with P_W and the power outage occurs.

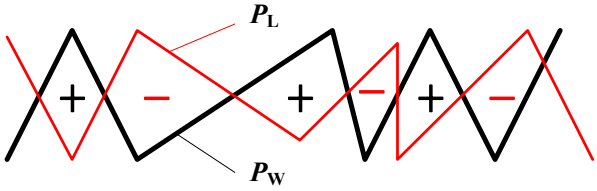

Fig. 2. The power mismatch between P_W and P_L

2.2. Primary sizing principles

The primary concern of most SWP system users is to ensure SWP systems to supply reliable power while incurring least overall cost. The sizing of SWP systems is to determine proper wind turbine size and battery capacity to allow SWP systems to provide reliable and cost-effective electricity to meet the load demand.

For the SWP system in Fig. 1, the input power P_W from the wind via the wind turbine can be modelled [3] as

$$P_W = \begin{cases} 0 & v < v_i \text{ or } v > v_o \\ 0.5\rho A_W v^3 C_P \eta_W & v_i \le v \le v_r \\ 0.5\rho A_W v_r^3 C_P \eta_W & v_r < v < v_o \end{cases} \quad (1)$$

where v represents the wind speed, the cut-in wind speed $v_i \in [1.5, 3.5]$ m/s, the rated wind speed $v_r \in [12, 17]$ m/s, the cut-off wind speed v_o is set as 25 m/s, the air density ρ is about 1.225 kg/m^3 at sea level and at 15 ℃, A_W presents the blade swept area, and C_P is the power coefficient with maximum value C_{Pmax} =16/27≈0.593 [1].

To meet a given load demand P_L over a period of T, the size of the wind turbine should at least satisfy

$$\bar{P}_W = \frac{1}{T}\int_0^T P_W dt = m_W \cdot \alpha \cdot \gamma \cdot \bar{P}_L > \bar{P}_L = \frac{1}{T}\int_0^T P_L dt \quad (2)$$

where $\bar{P}_W$ and $\bar{P}_L$ are the required average wind power generation and the given average load demand, respectively; $\alpha \ge 1$ is the size factor; $\gamma \ge 1$ is the correction coefficient to account for the transmission power losses; and $m_W \ge 1$ is the margin factor of the wind turbine size to account for the wind speed variations. Note that the coefficients α, γ and m_W are not considered in conventional sizing method [1] [29], i.e. $\alpha = \gamma = m_W = 1$.

Therefore, for a given load demand, the required wind turbine size can be determined by the annual wind speed v using Eqs. (1) and (2). Apparently, the measurement of wind speed is the most crucial factor in the design of SWP systems, especially in the sizing of wind turbine. Considering the wind power variations, the margin factor $m_W \ge 1$ is included to account for the deficient wind power generation.

Due to the generation-load mismatch power, the transmission efficiency η_T from P_W to P_L can be calculated as [31]

$$\eta_T = \beta + (1-\beta)\cdot\eta_B \quad (3)$$

where β denotes the ratio of wind power generation directly transferred to the load via electricity bus, and the other (1-β) via the battery. For a SWP system, it is reasonable to assume $\beta = 0.5$ due to the randomness of wind power. Without loss of generality, the correction coefficient $\gamma = 1/\eta_T \approx 1.1$ is introduced to compensate the mismatch transmission loss.

As an energy storage device, the battery bank is utilized to smooth the generation-load mismatch power $\Delta P = P_W - P_L$ like Fig. 2. The active battery bank capacity B_{ac} in hours [31] can be expressed as

$$B_{ac} = m_B \cdot B_n \cdot DoD \cdot \eta_B \cdot \left(1/\bar{P}_L\right) \quad (4)$$

where B_n is the nominal battery capacity in kWh, DoD is the depth of discharge of the battery, m_B is the margin factor of the battery capacity, and $\bar{P}_L$ is the average load demand in kW. Considering the inter-annual variations of the generation-load mismatch power, the margin factor $m_B \ge 1$ is utilized to account for the worst power fluctuation. However, given the randomness and uncontrollability of wind power and load power consumption, it remains a challenging issue to determine proper battery capacity to guarantee the power supply reliability while incurring least overall cost [1, 9-15, 29].

For the optimal design of SWP systems, the impacts of wind power variability on the sizing of the battery and the wind turbine should be taken into consideration. As a subsequent step, it is essential to develop an effective way to quantitively measure the variability of wind power.

3. A new measure of wind power variability

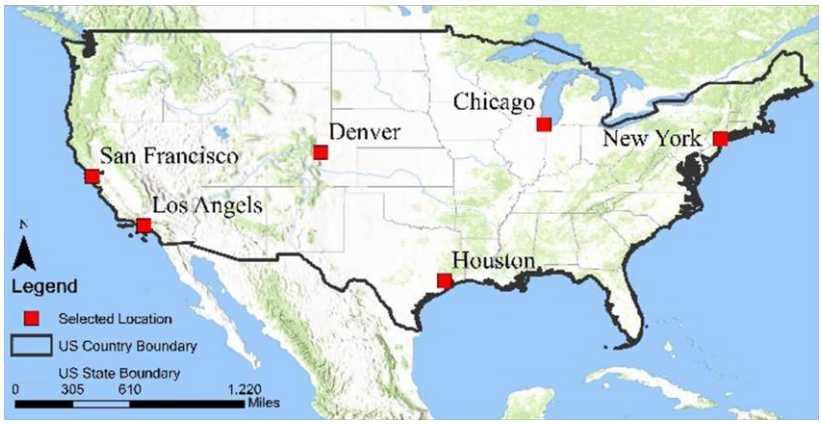

Fig. 3. Locations of the six sites selected for this research.

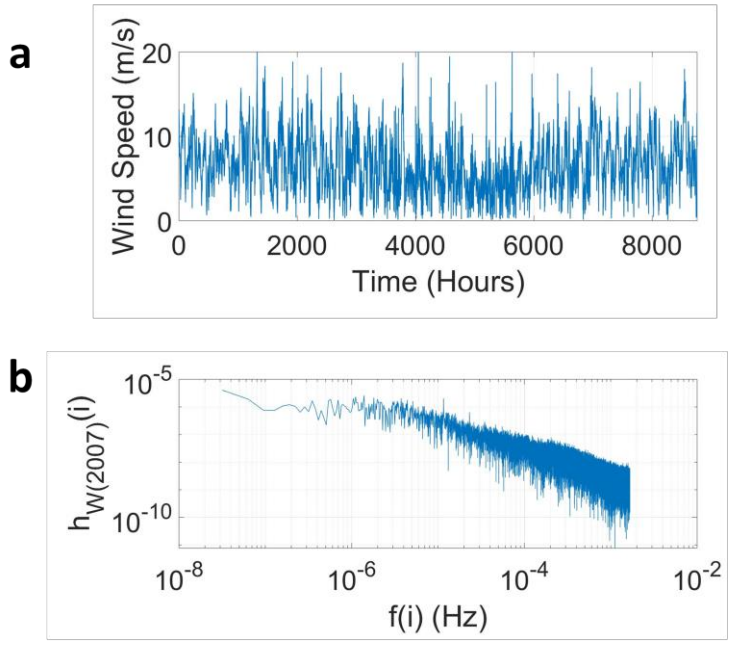

Fig. 4. Annual wind data of Chicago in 2007 (a) Wind speed, (b) Power spectrum of normalised wind power generation

For the analysis of wind variability, the real wind speed data with a sampling time interval T_S = 5 minutes are obtained from the Wind Integration National Dataset (WIND) Toolkit [30], which includes meteorological conditions for more than 126,000 locations in the continental United States for the years 2007–2012. As shown in Fig.3, six distantly distributed sites in New York, Chicago, Houston, Denver, Los Angeles and San Francisco are selected to ensure the proposed method can be utilised in extensive geographical context. Fig. 4a shows an example of the collected annual wind speed data at Chicago in 2007 where $v_{(n)}(i) \geq 0$ (i = 1, 2, …, 105120 and the subscript n is the year). The corresponding output power generated by a wind turbine, $P_{W(n)}(i) \geq 0$ can be obtained using Eq. (1) with v_i =2 m/s, v_r =14 m/s, v_o=25 m/s, ρ =1.225 kg/m^3 and C_P =0.593.

For further analysis, the normalized annual wind power/energy generation data $P_{N(n)}(i)$ with sampling time interval T_S = 5 minutes for the year n at one site can be expressed as

$$\left\{ P_{N(n)}(i) = \frac{P_{W(n)}(i)T_S}{\sum_{i=1}^{105120} P_{W(n)}(i)T_S} = \frac{P_{W(n)}(i)}{\sum_{i=1}^{105120} P_{W(n)}(i)} \right\} \tag{5}$$

In spite of the stochastic intermittence, both $P_{W(n)}(i)$ and $P_{N(n)}(i)$ show quasi-periodic features at different timescale. For instances, the peaks of seasonal wind power production regularly occur during a specific season across years at all sites. Therefore, using FFT, the quasi-periodic $P_{N(n)}(i)$ in the time domain can be transformed into a set of normalized wind power harmonics $0< h_{W(n)}(i) <1$ (i=1,2, …, 52559) and the DC power component $h_{w(n)}(0)$=1/52560 with frequency $f(0) = 0$ Hz in the frequency domain. Fig. 4 (b) shows the spectrum of annual wind power harmonics without the DC component, where f(i) denotes the corresponding frequency of the i-th order harmonics. It can be observed in Fig. 4 (b) that the profile of $h_{W(n)}(i)$ decreases with the increase of frequency in the band of $(4\times10^{-6}, 1.67\times10^{-3})$ Hz or (0.167, 69) hours.

3.1. Inter-annual wind energy variation

From Eqs. (1) and (2), the wind turbine size is mainly determined by the wind speed in the time domain. In addition to the size factor α, the margin factor m_W is needed to account for the worst inter-annual variations of wind power in the sizing of the wind turbine. In the time domain, the inter-annual wind energy variations for years 2007-2012 at each site with corresponding margin factor m_W of wind turbine size can be expressed as

$$\begin{cases} E_W(n) = \sum_{i=1}^{105120} P_{W(n)}(i)T_S \\ I_W(n) = E_W(n) / \left(\sum_{i=2007}^{2012} E_W(i) / 6 \right) \\ v_{avg} = \left(\sum_{n=2007}^{2012} \left(\sum_{i=1}^{105120} v_{(n)}(i) / 105120 \right) \right) / 6 \\ \delta_{I\max} = \max(I_W(n)) - 1 \\ \delta_{I\min} = \min(I_W(n)) - 1 \\ m_W = 1 / \left(1 + \delta_{I\min}\right) \end{cases} \tag{6}$$

where $E_W(n)$ is the total annual wind power generation for the year n; $I_W(n)$ is the ratio of the total wind energy in the year n to the average for the years 2007-2012, v_{avg} is the average wind speed for the years 2007-2012, $\delta_{I\max}$ and $\delta_{I\min}$ are the upper and bottom bounds of $I_W(n)$, and margin factor m_W is used to account for the worst inter-annual variations of wind speed for determining the size of wind turbine in Eq. (2).

Table 1 gives the inter-annual wind energy variations at the six sites for the years 2007-2012. It can be seen that, (i) the wind speed significantly varies from site to site; (ii) m_W significantly varies from site to site. From the data listed in Table 1, it is not difficult to know that, Los Angeles have the poorest wind source for power generation.

Table 1
Inter-annual wind power variations at the six sites for the years 2007-2012.

Location Name	$I_W(n)$						$\delta_{I\max}$	$\delta_{I\min}$	v_{avg} (m/s)	m_W
	2007	2008	2009	2010	2011	2012				
San Francisco	1.03	1.00	1.01	0.97	0.95	1.03	+3%	-5%	7.91	1.05
Los Angeles	1.07	0.97	0.83	1.14	1.04	0.95	+14%	-17%	4.72	1.20
Denver	1.04	1.02	0.91	0.96	1.01	1.05	+5%	-9%	6.75	1.09
Houston	1.14	0.80	1.04	1.00	1.14	0.89	+14%	-20%	6.51	1.25
Chicago	1.04	1.04	0.95	0.95	1.04	0.98	+4%	-5%	7.71	1.05
New York	0.98	0.98	1.02	1.13	0.97	0.93	+13%	-7%	7.31	1.08

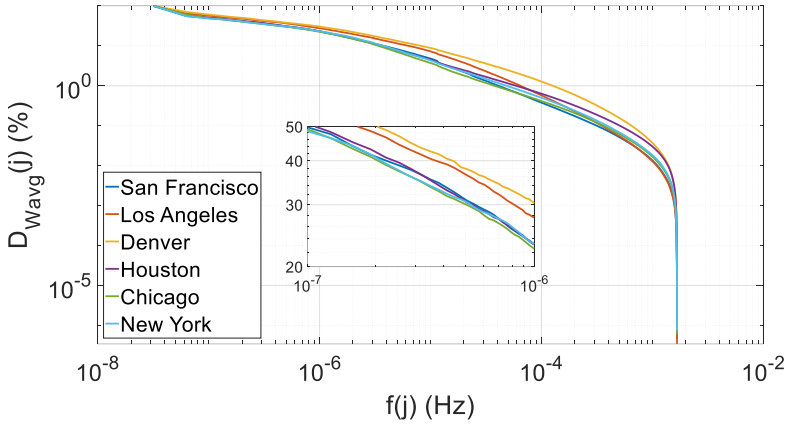

Fig. 5. $D_{Wavg}(j)$ with frequency $f(j)$ at the six sites.

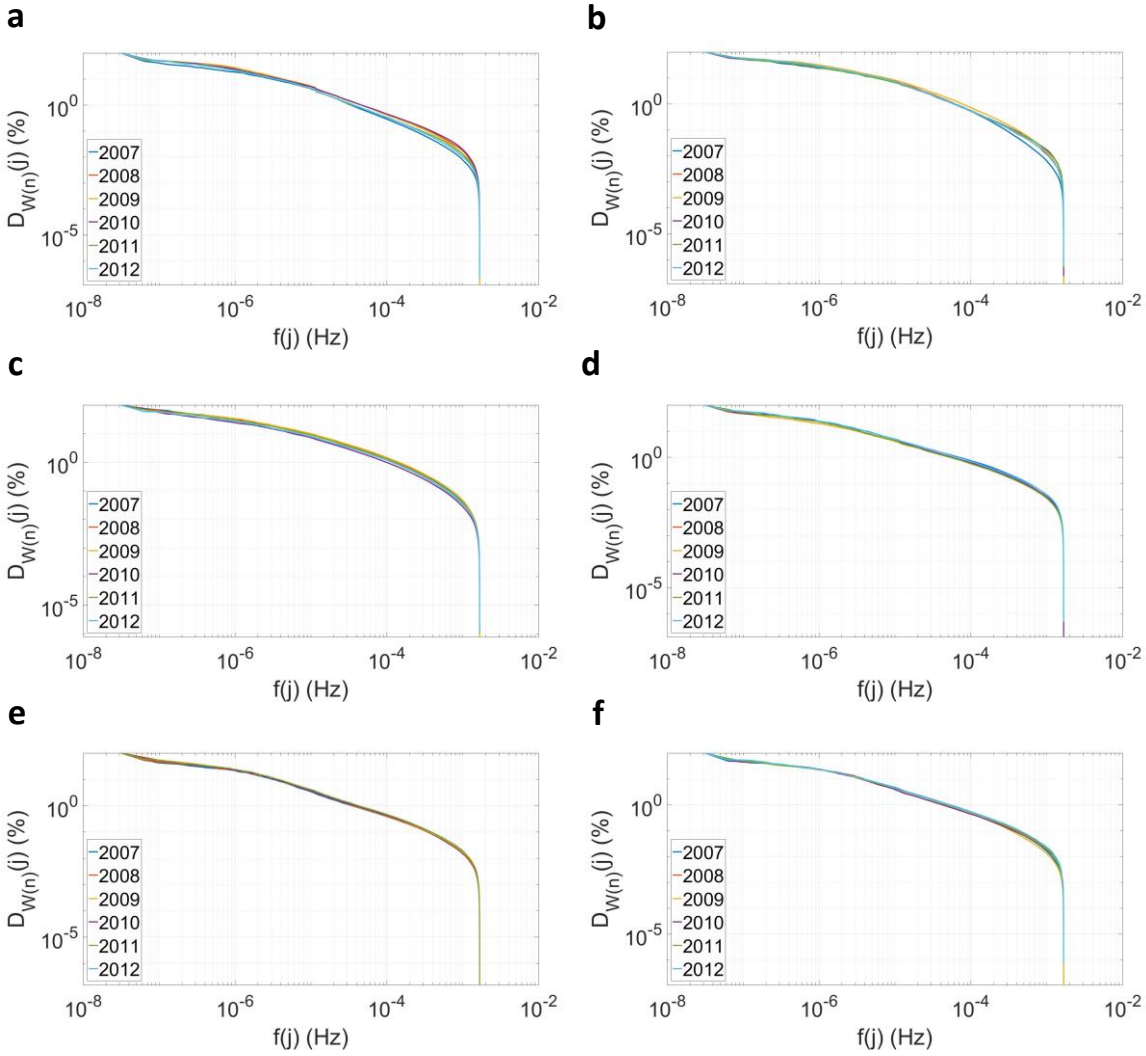

Fig. 6. $D_{W(n)}(j)$ with frequency $f(j)$ for the years 2007-2012 at (a) San Francisco, (b) Los Angeles, (c) Denver, (d) Houston, (e) Chicago, (f) New York.

3.2. Wind power distribution in the frequency domain

In view of the quasi-periodic characteristics of wind power, annual wind power fluctuation can be represented as a combination of sinusoidal power harmonics and DC power component. Thus, the wind power fluctuations can be considered as a power harmonics source. Hence the mitigation of wind power fluctuations can be treated as the energy filtering of power

harmonics. Then, a cumulative energy distribution index $D_{W(n)}(j)$ for annual wind power generation in the frequency domain is defined as below

$$\begin{cases} e_{W(n)}(i) = h_{W(n)}(i)T(i)/\sqrt{2} \\ D_{W(n)}(j) = \dfrac{\sum_{i=j}^{52559} e_{W(n)}(i)}{\sum_{i=1}^{52559} e_{W(n)}(i)} \times 100\% \\ D_{Wavg}(j) = \sum_{n=2007}^{2012} D_{W(n)}(j)/6 \end{cases} \tag{7}$$

where $e_{W(n)}(i)$ with i =1,2, …, 52559 denotes the energy of the i-th order wind power harmonics for the year n; $T(i) = 1/f(i)$ is the corresponding period of the i-th order wind power harmonics of frequency $f(j)$; $D_{W(n)}(j)$ with j = 1,2, …, 52559 denotes the ratio of the wind energy in the frequency band of $[f(j), 1.67\times10^{-3}]$ Hz to the total annual wind energy for the year n, and $D_{Wavg}(j)$ is the average of $D_{W(n)}(j)$ over the study period. A higher $D_{W(n)}(j)$ implies a larger capacity of battery bank is needed to dampen the wind power variability in the frequency range of $[f(j), 1.67\times10^{-3}]$ Hz; and vice versa.

Fig. 5 shows that, all $D_{Wavg}(j)$ at the six sites are close to each other with noticeable differences among each other in the high frequency band of $(1\times10^{-6}, 1.67\times10^{-3})$ Hz or (0.167, 278) Hours, and all $D_{Wavg}(j)$ increase smoothly with the decrease of frequency $f(j)$. It implies that, a higher $D_{Wavg}(j)$ means that, a low-pass energy filter with the bandwidth of $f(j)$ Hz could reduce more wind power fluctuations.

Fig. 6 shows that, all $D_{W(n)}(j)$ at each site almost overlap each other, but except with small but noticeable variations in the frequency band of $(1\times10^{-5}, 1.67\times10^{-3})$ Hz at Los Angeles and San Francisco. The high degree of similarity among all $D_{W(n)}(j)$ at each site clearly demonstrates that, the energy distribution of annual wind power at each site is QTI. In other words, the wind power variability at each site can be considered to be QTI in the frequency domain.

3.3. Fluctuation factor of annual wind power

Being considered as a power harmonic source, the fluctuation of annual wind power can be characterized by using the total harmonic distortion of wind power relative to the constant DC power component. Consequently, a fluctuation factor of annual wind power with corresponding margin factor m_B of the battery capacity is defined as

$$\begin{cases} F_W(n) = \sqrt{\sum_{i=0}^{52559} \left(\dfrac{h_{W(n)}(i)}{h_{W(n)}(0)} \right)^2} \\ F_{Wavg} = \sum_{n=2007}^{2012} F_W(n)/6 \\ \delta_{F\max} = \max(F_W(n))/F_{Wavg} - 1 \\ \delta_{F\min} = \min(F_W(n))/F_{Wavg} - 1 \\ m_B = 1 + \delta_{F\max} \end{cases} \tag{8}$$

where the fluctuation factor of wind power for the year n is denoted as $F_W(n)$, F_{Wavg} is the average value of $F_W(n)$ for the years 2007-2012, $\delta_{F\max}$ and $\delta_{F\min}$ are the upper and lower bounds of $F_W(n)$, and the margin factor m_B is used to account for the worst wind power fluctuation in the sizing of battery.

Table 2
Fluctuation rates of wind power at the six sites for the years 2007-2012.

Location	$F_W(n)$						F_{Wavg}	$\delta_{F\max}$	$\delta_{F\min}$	m_B
	2007	2008	2009	2010	2011	2012				
San Francisco	1.93	1.97	1.97	1.98	2.04	1.96	1.98	+3.0%	-2.5%	1.03
Los Angeles	4.37	4.21	4.31	4.18	4.16	4.66	4.32	+7.9%	-3.7%	1.08
Denver	2.68	2.61	2.71	2.72	2.67	2.60	2.67	+1.9%	-2.6%	1.02
Houston	2.10	2.05	1.97	1.94	1.87	2.08	2.00	+5.0%	-6.5%	1.05
Chicago	2.00	2.01	2.03	2.05	2.02	2.03	2.02	+1.5%	-1.0%	1.02
New York	2.10	2.18	2.15	2.03	2.21	2.20	2.15	+2.8%	-5.6%	1.03

According to Eq. (8), for a constant DC power, i.e. $h_{W(n)}(0) > 0$ and $h_{W(n)}(i) = 0$ (i = 1, 2, …, 52559), $F_W(n) = 1$; otherwise power harmonics with $h_{W(n)}(0) > 0$ (i = 1, 2, …, 52559) would yield a larger $F_W(n) > 1$. That means that an intensive power fluctuation with more incorporated power harmonics will lead to a large $F_W(n)$. Therefore, $F_W(n)$ can be used to indicate the wind power variability in the frequency domain. Table 2 lists the values of $F_W(n)$ at the six sites for the study period. It can be seen that, in terms of the average fluctuation factor F_{Wavg}, taking the inter-annual variations $\delta_{F\max}$ and $\delta_{F\min}$ into consideration, the six sites can be ranked Los Angeles > Denver > New York ≈ Chicago ≈ Houston ≈ San Francisco. F_{Wavg} at Los Angeles is around two times of those at other five sites, and the inter-annual variation $\delta_{F\max} = 7.9\%$ at Los Angeles is the highest among the six sites. That implies that, the most fluctuated wind power might lead to the poorest power supply reliability of SWP systems at Los Angeles.

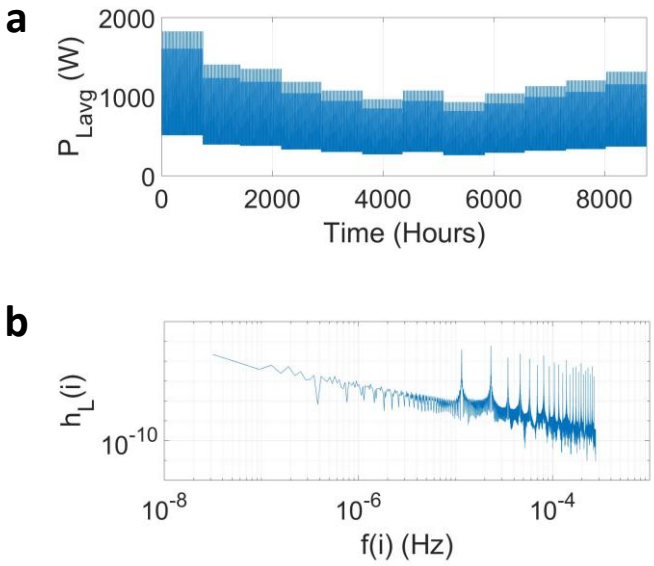

Fig. 7. A typical average annual residential power consumption (a) Load data, (b) Load power spectrum.

4. Impacts of wind power variability

4.1. Generation-load mismatch power

As mentioned in Section 2, it is the generation-load mismatch power instead of only the wind power, which causes power outages and then reduces the power supply reliability of SWP systems. In practice the increment of the battery capacity and the enlargement of the wind turbine size could provide two feasible ways to mitigate the mismatch power.

Fig. 7 gives a typical average annual residential load consumption P_{Lavg} with $\bar{P}_L = 518.26$ W and its normalized power spectrum. Like quasi-periodic wind power, the residential load demand also changes daily, weekly and seasonally. For instance, as shown in Fig. 7, the daily load consumption reaches its peak value in both morning and evening, and the monthly load consumption reaches its peak value in the winter. Note that Fig. 7 indicates that high degree of periodicity of the load demand data leads to spikes at specific harmonic frequencies above 9×10^{-6} Hz. In comparison, the energy distribution of wind power shown in Fig. 4 is of much higher degree of randomness. In view of the quasi-periodic characteristics of both the wind power and the load demand, the annual generation-load mismatch power $\Delta P = P_W - P_L$ can be also represented as a combined of power harmonics and a DC power component.

Likewise, using FFT, the annual mismatch power data $\Delta P(i) = P_W(i) - P_L(i)$ can be further transformed into a set of normalized mismatch power harmonics with $0 \le h_{M(n)}(i) \le 1$ (i=0,1, 2, …, 52559 and n is the year). Being enlightened from [26], the energy data $e_{M(n)}(i)$ of the i-th order mismatch power harmonics can be calculated as

$$\begin{cases} e_{M(n)}(i) = h_{M(n)}(i)T(i)/\sqrt{2} \\ e_{Mavg}(i) = \sum_{n=2007}^{2012} e_{M(n)}(i)/6 \end{cases}, \quad i = 1,2,...,52559 \tag{9}$$

Fig. 8 gives that the energy spectrums of average annual wind power e_{Wavg}, the average annual mismatch power e_{Mavg} and the average annual load consumption power e_L in the case in the case of $\bar{P}_W = m_S \cdot \alpha \cdot \gamma \cdot \bar{P}_L$ with α = 1 and γ = 1.1 and corresponding m_W listed in Table 1. It should be noted that average wind power data and average mismatch power for the study period was used to calculate the energy harmonics data in this case. It can be seen from Fig. 8 that, the mismatch energy harmonics data $e_{Mavg}(i)$ with insignificant spikes almost overlap with the wind energy harmonics data $e_{Wavg}(i)$ at each site, but is well above the load consumption energy harmonics $e_L(i)$. That implies that the wind power fluctuation dominates the mismatch power of SWP systems. Therefore, the mitigation of the mismatch power of SWP systems can be simply considered as the low-pass filtering of wind power harmonics.

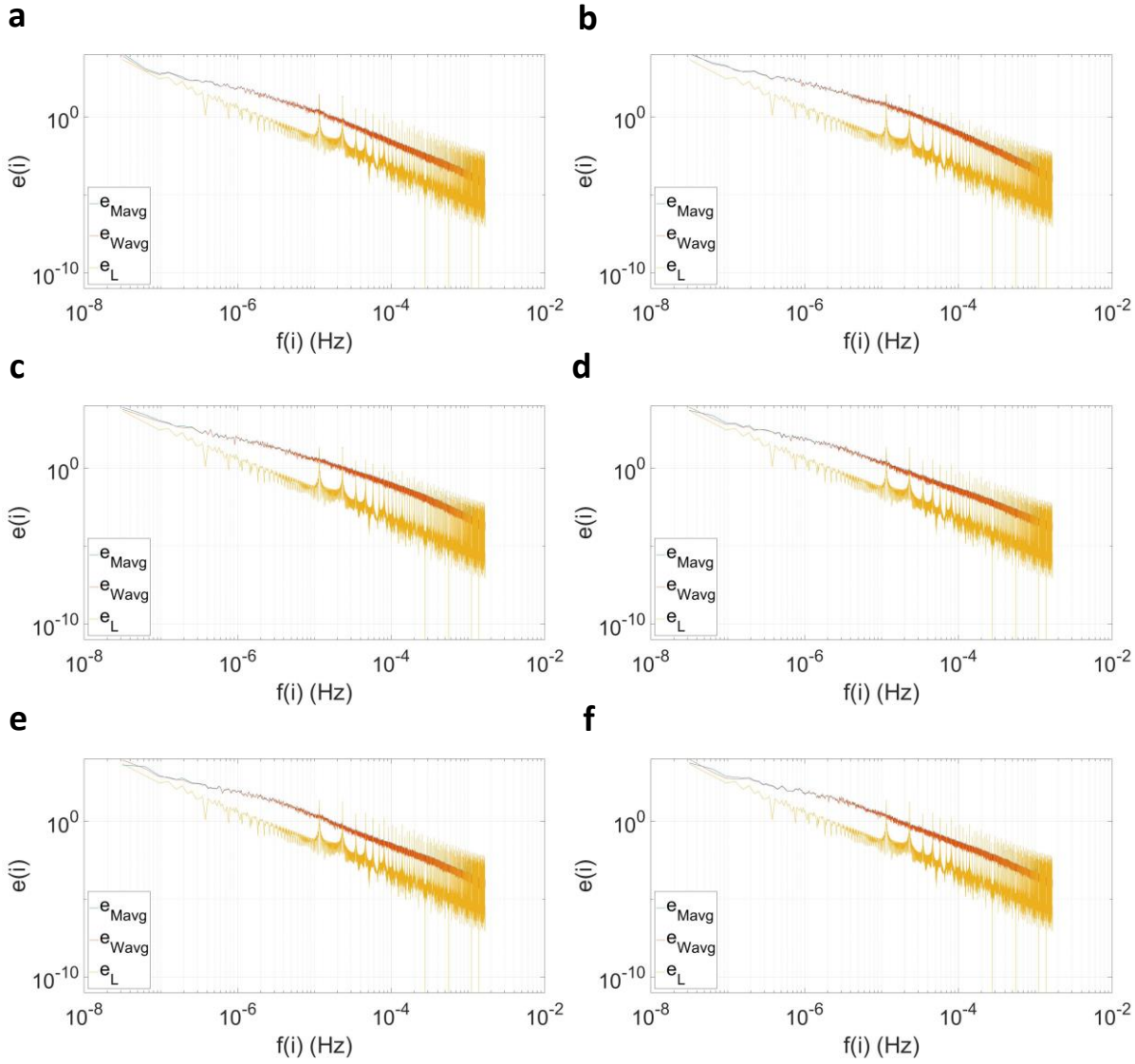

Fig. 8. Energy spectrum of average annual wind power, average annual mismatch power and average annual load demand from 2007 to 2012 at (a) San Francisco, (b) Los Angeles, (c) Denver, (d) Houston, (e) Chicago, (f) New York.

4.2. Battery capacity

Based on the above analysis, the battery energy storage can be modeled as a low-pass energy filter. Fig. 9 shows a model of energy filter for the battery. As shown in Fig. 9, if the *i*-th mismatch power harmonics $h_{M(n)}(i)\sin\left(2\pi t / T(i) + \varphi(i)\right)$ with $T(i)$ and $0 \le \varphi(i) \le 2\pi$ being the period and phase angle of the harmonics respectively, can be filtered out by the battery bank, the active battery capacity B_{ac} should be large enough to accommodate the energy fluctuation $e_{M(n)}(i)$ caused by *i*-th order mismatch power harmonics.

From Fig. 8, it can be seen that the profile of $e_{M(n)}(i)$ monotonously decreases with the increase of frequency. Therefore, if B_{ac} is large enough to filter out i-th order mismatch power harmonics, the battery would be able to filter out higher order mismatch power harmonics. It implies that, B_{ac} actually corresponds to the bandwidth of the low-pass energy filter. Furthermore, because the wind power fluctuation dominates the mismatch power, the mismatch power mitigation of SWP systems can be simply considered as the low-pass filtering of only wind power harmonics. Therefore, according to the similarity among the wind energy distribution at all six sites shown in Fig. 5 and Fig. 6, it is reasonable to anticipate all batteries in the SWP systems at six sites might behave similar low-pass filtering property - the power supply reliability might quasi-linearly increase with the growth of B_{ac} in all SWP systems at six sites. In addition, based on the energy distribution analysis shown in Fig.5, a higher $D_{Wavg}(j)$ means that, a low-pass energy filter of battery bank with the same active capacity B_{ac} could more efficiently reduce the wind power fluctuations and then more rapidly improve the power supply reliability. For instance, the power supply reliability of the SWP system at Denver might increase with the fastest rate in the frequency range of (1×10^{-6}, 1.67×10^{-3}) Hz because $D_{Wavg}(j)$ there is the highest among all six sites.

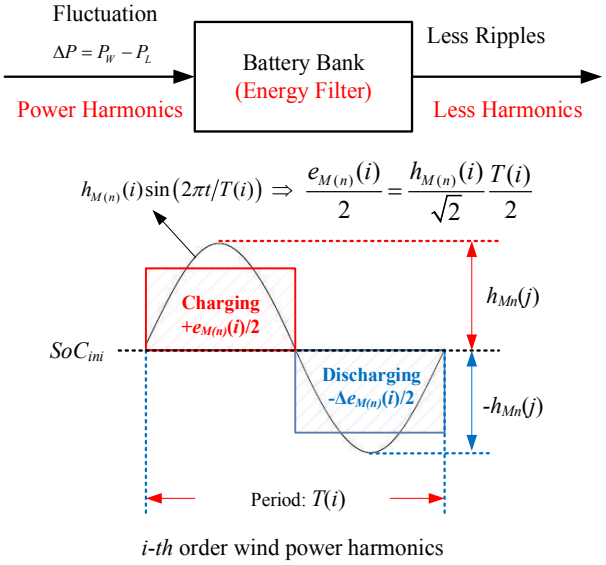

Fig. 9. A model of low-pass energy filter for the battery bank

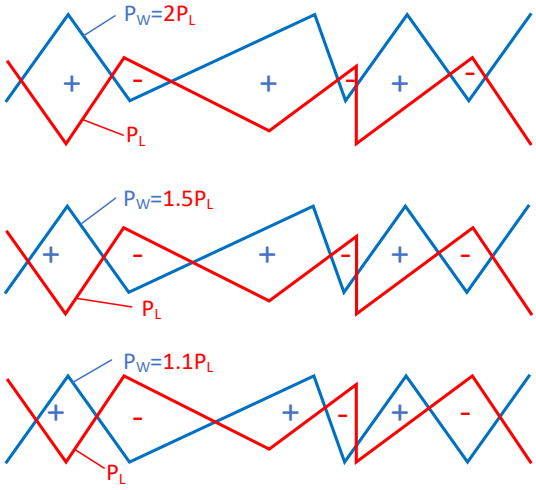

Fig. 10. The power mismatch of SWP systems with various wind turbine sizes.

4.3. Wind turbine size

Fig. 10 shows the mismatch power of SWP systems with various wind power generator capacity. The wind turbine size actually corresponds to the wind power generation capacity. It can be clearly seen from Fig. 10 that, the increase of wind turbine size could reduce the mismatch area labelled with '-', that is to say, a larger wind turbine size could allow the wind

power to effectively fill the deficit mismatch power $\Delta P = P_W - P_L < 0$ and remarkably reduce the power outages of SWP systems. That also implies that, with a given battery capacity, the power supply reliability of the SWP systems might monotonously increase with the increase of wind turbine size.

4.4. Power supply reliability

As shown in Fig. 2 and 10, the deficit generation-load mismatch power $\Delta P = P_W - P_L < 0$ will cause power outages and reduce the power supply reliability of SWP systems. The power supply reliability is a key factor in the optimal sizing of SWP systems. To evaluate the power supply reliability of SWP systems, the reliability factor R_W is defined as [32]

$$R_W = \left(1 - T_{out}/T\right) \times 100\% \tag{10}$$

where T_{out} is the total power outage time. A large R_W indicates a high power supply reliability, and vice versa.

Six SWP systems having the same residential load demand shown in Fig. 7, are configured for the six sites. When $\overline{P}_W = m_S \cdot \alpha \cdot \gamma \cdot \overline{P}_L$ with $\alpha = 1$ and $\gamma = 1.1$ and corresponding m_W listed in Table 1 at the six sites, the required wind turbine size at the six sites listed in Table 3 are calculated using Eqs. (1) and (2) with v_i =2 m/s, v_r =14 m/s, v_o=25 m/s, ρ =1.225 kg/m^3 and C_P =0.593.

Table 3
Wind turbine size and average wind speed.

Location Name	Swept Area of Wind Turbine A_W (m^2)	Average Wind Speed v_{avg} (m/s)
San Francisco	3.80	7.91
Los Angeles	21.65	4.72
Denver	6.74	6.75
Houston	8.40	6.51
Chicago	3.87	7.71
New York	4.56	7.31

The real wind speed data from WIND for the study period at each site have been employed to calculate the size of the corresponding wind turbine using Eqs. (1) and (3). Table 3 indicates that, in terms of either the mean wind power density in kW·m^{-2} or the average wind speed for the study period, taking the inter-annual variations of wind power listed in Table 1 into consideration, the sizes of the wind turbine follow the ranking San Francisco ≈ Chicago < New York < Houston ≈ Denver < Los Angeles. Hence, the wind speed at San Francisco and Chicago allows the SWP systems to produce wind power to meet the load consumption while incurring the lowest cost of wind turbine, while the one at Los Angeles incurs the highest cost of wind turbine.

Table 4
Average power supply reliability R_{wavg} with $B_{ac} = 10^0$, 10^1 and 10^2 hours and $\alpha = 1.0$, 1.5, and 2.0.

Size factor	**α = 1.0**			**α = 1.5**			**α = 2.0**		
B_{ac} (Hours) / **R_{Wavg}(%)**	10^0	10^1	10^2	10^0	10^1	10^2	10^0	10^1	10^2
San Francisco	56	68	78	64	76	88	69	81	92
Los Angeles	41	51	63	46	60	75	50	67	85
Denver	47	62	76	54	72	90	59	78	94
Houston	60	71	84	69	80	95	74	86	98
Chicago	55	65	78	64	74	90	69	80	96
New York	55	65	78	64	75	91	69	81	97

Fig. 11 shows the simulation results of the dependence of the power supply reliability factor R_W on the active battery capacity B_{ac} and the wind turbine size factor α respectively: (i) with a given α, R_W quasi-linearly increases with the growth of B_{ac}, where the unit of B_{ac} is $\overline{P}_L \cdot hours$, abbreviated *Hours*; (ii) the lines of R_W against B_{ac} parallelly move up with the

growth of α; (iii) compared with Fig. 5, a higher cumulative energy distribution index $D_{Wavg}(j)$ would lead to a faster ramping rate of R_W against B_{ac}, e.g. R_W at Denver increases with the fastest rate among all six sites when B_{ac}≤100 hours.

Table 4 lists the values of R_{Wavg} of all six SWP systems with $B_{ac} = 10^0$, 10^1 and 10^2 *Hours* and α = 1.0, 1.5 and 2.0 respectively, where R_{Wavg} is the average value of R_W for the study period shown in Fig. 11. Table 4 indicates that, with the same B_{ac} and α, taking the inter-annual variations of R_W in Table 1 into consideration, the ranking of the six SWP systems are Los Angeles < Denver < New York ≈ Chicago ≈ Houston ≈ San Francisco in terms of the R_{Wavg}. It can be seen from Table 2 that, the six sites are reversely ranked Los Angeles > Denver > New York ≈ Chicago ≈ Houston ≈ San Francisco with respect to the average fluctuation factor F_{Wavg}. Obviously, the ranking of R_{Wavg} of the six SWP systems is reversely consistent with F_{Wavg} of wind power. The consistency between R_W and F_{Wavg} indicates the high degree of dependence between these two indictors – with the same B_{ac} and α, the higher F_{Wavg} is, the lower R_W is. The proposed fluctuation factor in Eq. (8) provides a useful quality index to the wind resource assessment for the development of the SWP systems.

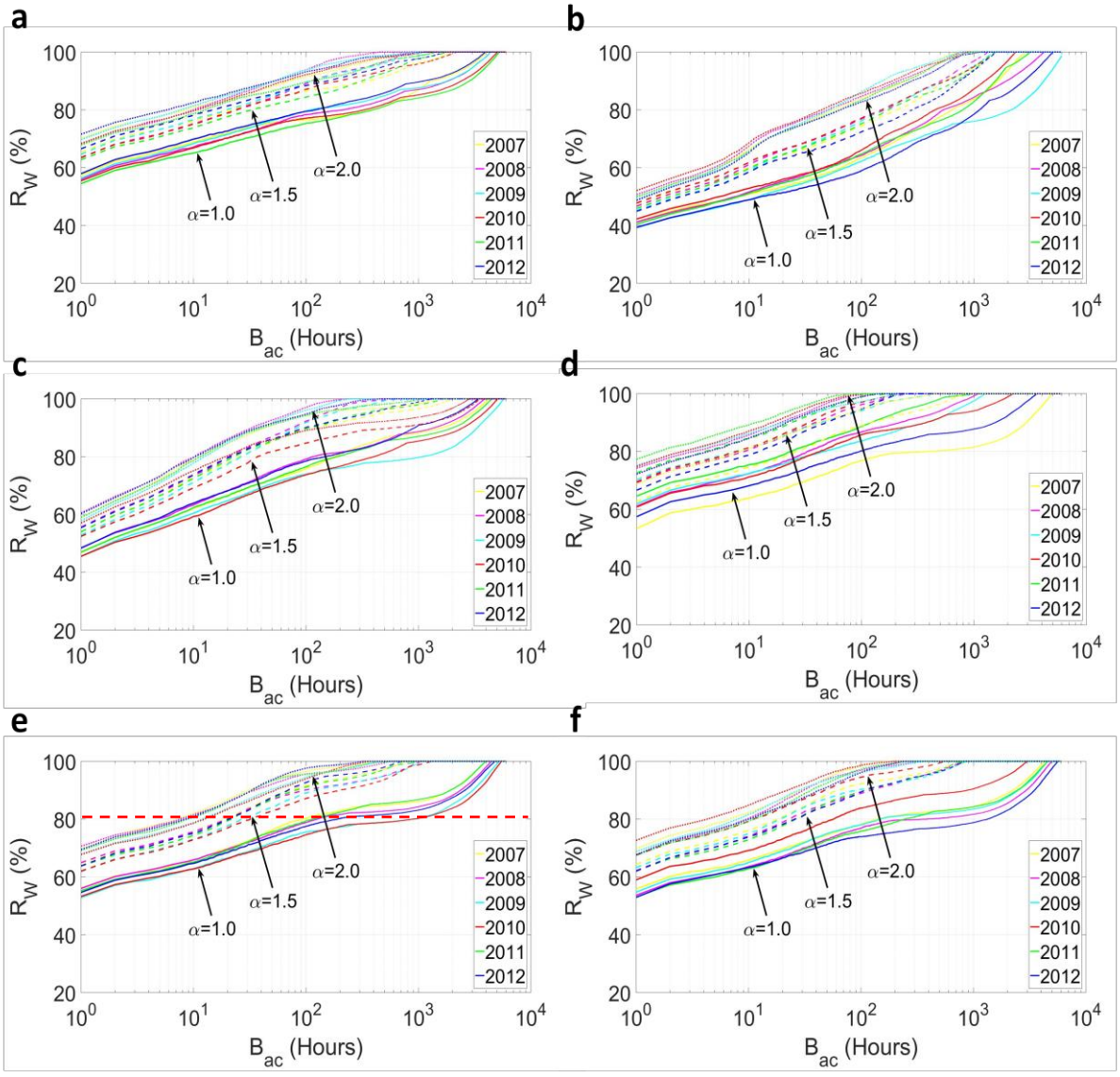

Fig. 11. Power supply reliability R_W against active battery capacity B_{ac} with α = 1.0, 1.5, 2.0 for the study period at (a) San Francisco, (b) Los Angeles, (c) Denver, (d) Houston, (e) Chicago, (f) New York.

Generally speaking, compared with the analysis results in Section 3, the simulation results shown in Fig. 11 affirms the validity of the new measure of wind power variability. Since the wind power variability at one site can be treated as a QTI power harmonics source in the frequency domain, the dependence of R_W on B_{ac} and α shown in Fig. 11 can be also treated as QTI responses, which can be used as datasheet for simplifying the optimal sizing of the battery and the wind turbine.

5. Case study

The power supply reliability and cost-effectiveness are two primary concerns of most SWP system owners. One typical design scenario for the optimal sizing of SWP systems is to build the most cost-effective system subject to various constraints, especially the constraints on the power supply reliability. The most common objective of optimal sizing of SWP systems is to minimize the system cost in \$·kWh^{-1} while satisfying the requirement of power supply reliability, whose function can be described as [4, 17]

$$COE = \min\left\{\frac{\overbrace{C_{Wi}\cdot A\cdot\alpha\cdot\gamma\cdot m_W + C_{Wm}\cdot Operation\ period}^{\text{cost of wind turbine}}}{R_W\cdot\int P_L dt} + \frac{\overbrace{(C_{Bi}+C_{Bm})\cdot B_n\cdot m_B}^{\text{cost of battery bank}}}{R_W\cdot\int P_L dt}\right\} \tag{11}$$

where COE in \$·kWh^{-1} is the abbreviation of Cost of Energy; C_{Wi} and C_{Bi} denote the initial capital cost of wind turbine in \$·m^{-2} and battery bank in \$·kWh^{-1} respectively; C_{Wm} and C_{Bm} denote the maintenance cost of PV panel in \$·years^{-2} and battery bank in \$·kWh^{-1} respectively. Note that the impacts of the wind power variability on the sizing of the wind turbine and the battery are included in the cost function in Eq. (11).

Table 5
Details of wind turbine and Lead-acid battery.

Wind turbine		Lead-acid battery		*DoD* (%)	Cycle life
C_{Wi}	1000 \$/m^2	C_{Bi}	225 \$/kWh	10	6200
C_{Wm}	100 \$/years	C_{Bm}	0 \$/m^2	20	5700
Life	20 years	Life	*DoD*-dependent	50	1800
η_W	90%	η_B	81%	80	600
				100	425

Table 6
Most cost-effective final battery capacity B^*.

B_{ac} (hours)	*DoD* (%)	N_B	B^* (kWh)
1 ~11	50	1	$3.03B_{ac}\bar{P}_L$
12 ~ 19	100	2	$3.03B_{ac}\bar{P}_L$
20 ~ 32	80	1	$1.89B_{ac}\bar{P}_L$
≥ 33	100	1	$1.51B_{ac}\bar{P}_L$

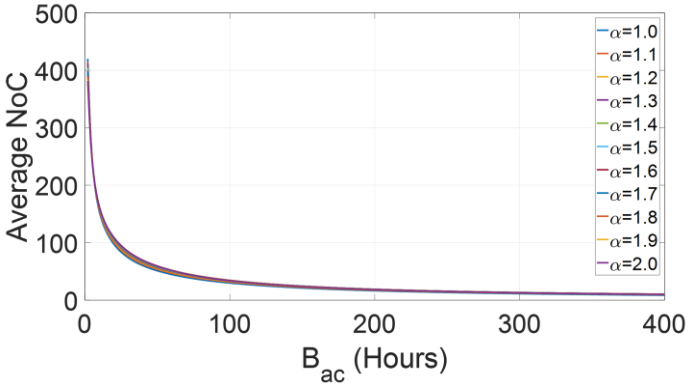

Fig. 12. Average *NoC* of the battery of the SWP system with $\alpha = 1 \sim 2$ for the years 2007-2012.

A case study of the optimal sizing of a SWP system in Chicago with residential load demand shown in Fig. 7 with annual $\bar{P}_L = 518.26$ W is presented to demonstrate the impacts of wind power variability. The sizing constraints for the minimization of the cost function in Eq. (11) can be specified as: $R_{W,min} \le R_{set} \le R_W < 100\%$, where $R_{W,\min}$ represents the minimum system reliability of SWP system operation ($R_{W,\min} = 55\%$ at Chicago, as shown in Fig. 11e) and R_{set} denotes the specification

objective, and $\alpha_{\max}$ and $B_{ac,\max}$ represent the limits of physical size (e.g. space, weight, …). In the case of $R_{set} \le R_{W.min}$, the optimal wind turbine size factor would be $\alpha = 1$, and no battery storage is needed. Note that, based on the dependence relationships of R_W vs. C_B and R_W vs. α shown in Fig. 11e, the sizing constraint zone is enclosed by a convex combination of quasi-straight lines, which might help simplify the sizing optimization of the SWP systems. For this case study, the specification objective of the SWP system is set as R_{set} = 80% and the life cycle being 6 years.

From Fig. 11e, it can be seen that, if $R_W \ge R_{set}$ =80%, the constraint of active battery capacity for the minimization of the cost function in Eq. (11) can be explicitly specified as 10 hours < B_{ac} < 1500 hours. Obviously, the explicit constraint of active battery capacity could lead to a significant reduction of computation in the optimal sizing.

Table 7
Cost of Energy (*COE*) with different wind turbine size factor and active battery capacity.

Battery Capacity		*COE* ($/kWh)										
DoD (%)	B_{ac} (hours)	α=1.0	α=1.1	α=1.2	α=1.3	α=1.4	α=1.5	α=1.6	α=1.7	α=1.8	α=1.9	α=2.0
50	≤10	n/a	n/a	n/a	n/a	n/a	n/a	n/a	n/a	n/a	n/a	0.027
50	11	n/a	n/a	n/a	n/a	n/a	n/a	n/a	n/a	n/a	n/a	0.028
100	12	n/a	n/a	n/a	n/a	n/a	n/a	n/a	n/a	n/a	0.028	0.028
100	13	n/a	n/a	n/a	n/a	n/a	n/a	n/a	n/a	n/a	0.029	0.029
100	14	n/a	n/a	n/a	n/a	n/a	n/a	n/a	n/a	0.029	0.029	0.030
100	15	n/a	n/a	n/a	n/a	n/a	n/a	n/a	n/a	0.030	0.030	0.030
100	16	n/a	n/a	n/a	n/a	n/a	n/a	n/a	0.030	0.030	0.031	0.031
100	17	n/a	n/a	n/a	n/a	n/a	n/a	n/a	0.031	0.031	0.031	0.032
100	18	n/a	n/a	n/a	n/a	n/a	n/a	n/a	0.031	0.032	0.032	0.033
100	19	n/a	n/a	n/a	n/a	n/a	n/a	n/a	0.032	0.033	0.033	0.033
80	20	n/a	n/a	n/a	n/a	n/a	n/a	**0.026**	0.027	0.027	0.027	0.028
80	21	n/a	n/a	n/a	n/a	n/a	n/a	0.027	0.027	0.027	0.028	0.028
80	22	n/a	n/a	n/a	n/a	n/a	n/a	0.027	0.027	0.028	0.028	0.028
80	23	n/a	n/a	n/a	n/a	n/a	n/a	0.027	0.028	0.028	0.028	0.029
80	24	n/a	n/a	n/a	n/a	n/a	0.027	0.028	0.028	0.028	0.029	0.029
80	25	n/a	n/a	n/a	n/a	n/a	0.028	0.028	0.028	0.029	0.029	0.030
80	26	n/a	n/a	n/a	n/a	n/a	0.028	0.029	0.029	0.029	0.030	0.030
80	27	n/a	n/a	n/a	n/a	n/a	0.029	0.029	0.029	0.030	0.030	0.030
80	28	n/a	n/a	n/a	n/a	n/a	0.029	0.029	0.030	0.030	0.031	0.031
80	29	n/a	n/a	n/a	n/a	n/a	0.030	0.030	0.030	0.031	0.031	0.031
80	30	n/a	n/a	n/a	n/a	0.030	0.030	0.030	0.031	0.031	0.031	0.032
≥ 80	≥ 31	≥ 0.105	≥ 0.048	≥ 0.036	≥ 0.030	≥ 0.030	≥ 0.031	≥ 0.031	≥ 0.031	≥ 0.031	≥ 0.032	≥ 0.032

Details of the wind turbine and lead-acid battery [33] are listed in Table 5. Noted that, the price of commercial wind turbine has a big difference because of the difference of specific configuration. According to the wind turbine price of Bergey, Jacobs, and Endurance's product [34, 35], C_{Wi} and C_{Wm} in $/m^2 can be reasonably assumed for the convenience of further calculations. Moreover, the cycle life of the lead-acid battery nonlinearly depends on *DoD* in practice. For instance, as shown in Table 5, if *DoD* = 10%, the battery capacity will fall under 80% of the original capacity after 6200 times complete charge/discharge cycles, while *DoD* = 20%, the cycle life will drop to 5700 times. It can be seen from Fig. 12 that, the Number of annual complete charge/discharge Cycles (*NoC*) of battery bank decreases with the growth of B_{ac}, while it doesn't change very much with $\alpha = 1 \sim 2$. Note that, since the battery capacity will fall under 80% of its original capacity after the cycle life of battery, the final battery capacity can be chosen as $B^* = B_n/80\% = 1.25B_n$ to guarantee the system reliability always meet the specific required reliability R_{set} over study period, where B_n is calculated by using Eq. (4). From Table 5 it can be seen that, if a large *DoD* is taken, the life cycle of battery bank might be shorter than 6 years, that is to say, the SWP system needs several sets of battery bank for sustaining its normal operation over 6 years. Based on Table 5 and Fig. 12, the most cost-effective final battery capacity B^* in our case study are figured out and listed in Table 6, where $B^* = 1.25N_B B_n = 1.25N_B B_{ac}\bar{P}_L / (DoD \cdot \eta_B \cdot m_B)$.

Based on Fig. 11e and Table 3-6, the results of the optimal sizing of the SWP system at Chicago are listed in Table 7. The minimum *COE* of 0.026 $·kWh^{-1} occurs at B_{ac} = 20 hours, *DoD* = 80%, and $\alpha = 1.6$. Therefore, taking the QTI impacts of

wind power variability into consideration, (i) according to Table 6, the final battery capacity would be chosen as $B^* = 1.89B_{ac}$ $\bar{P}_L \approx 19.60$kWh; (ii) according to Table 3, the selected wind turbine swept area is $\alpha \times A_W = 1.6 \times 3.87 \approx 6.19\text{m}^2$.

This case study indicates that the QTI responses shown in Fig. 11 enable us to quickly obtain the explicit constraint of battery capacity and then significantly reduce the computation for the optimal sizing of SWP systems. The complete process of the optimal sizing of SWP systems using the proposed approach is drawn as the flow chart shown in Fig. 13.

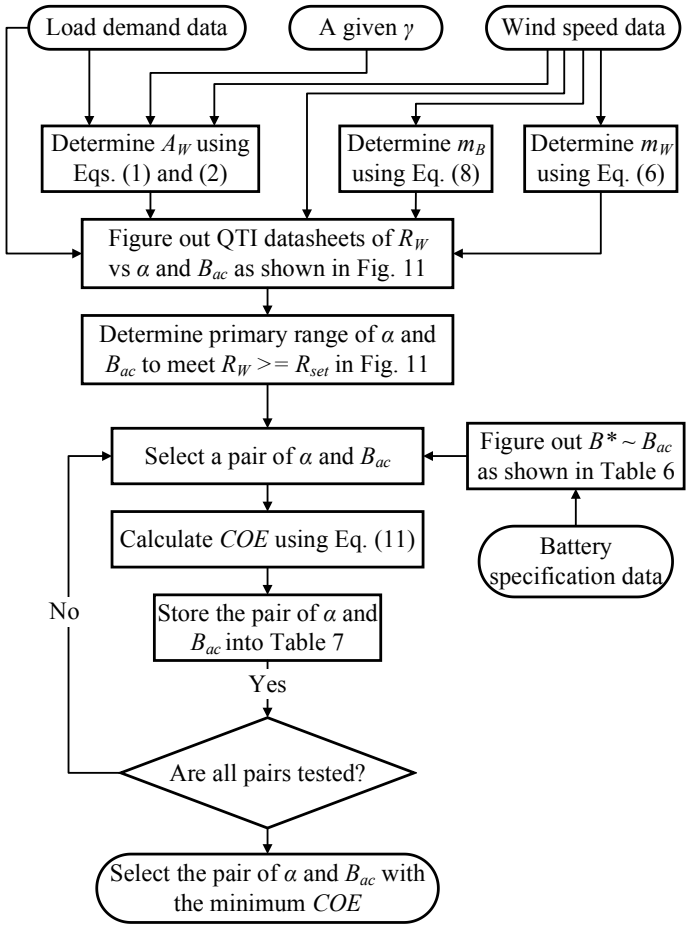

Fig. 13. Optimal sizing of SWP systems using the proposed approach

6. Conclusion

The variability of intermittent wind power has significant impacts on the power supply reliability and system costs of Standalone Wind Power (SWP) systems. This paper presented an attempt to measure the wind power variability and investigates the impacts of the wind power variability on the optimal sizing of the SWP systems. The proposed new measure of the wind power variability in the frequency domain, which includes a cumulative energy distribution index and a fluctuation factor, is applied to assess the wind speed data throughout six consecutive years from six far apart sites from latitude 0° to 50° across America. Based on the new measure of wind power variability, the impacts of wind power variability on the sizing of the battery and the wind turbine are investigated in the mitigation of wind power variability. Taking the impacts of wind power variability into consideration, big data simulations of the six SWP systems with the same residential load demand at the six sites were carried out to reveal the dependency between the sizing of the system components (i.e. the battery and the wind turbine) and the power supply reliability. In this context, a case study of optimal sizing of the SWP system at Chicago, was carried out to demonstrate the feasibility of the proposed methods, which aims is to minimize the system cost while satisfying the requirement of power supply reliability. It has been found from the study that

i) Big data based spectrum analysis of wind power and load power indicates that the wind power variability dominates the power fluctuation of SWP systems with residential loads in the case of $\overline{P}_W > \overline{P}_L$. The power fluctuation mitigation of SWP systems can be simply treated as the filtering of wind power harmonics.

ii) Big data based new measurement of wind power variability indicated that, the intermittent wind power in the time domain at one site is QTI in the frequency domain.

iii) A higher cumulative energy distribution index $D_{W\text{avg}}(j)$ is corresponding to a faster ramping rate of the power supply reliability R_W against active battery capacity B_{ac}.

iv) There is a high degree of consistency between the proposed fluctuation factor F_W of wind power and the power supply reliability R_W of the SWP systems - with the same B_{ac} and α, the higher F_{Wavg} is, the lower R_W is. The fluctuation factor can provide a useful quality indicator to the wind resources assessment for the development of SWP systems.

v) The dependence of R_W on B_{ac} and α of SWP systems can be considered as QTI responses, which can be used to quickly determine the explicit constraints of the minimization of the cost function and significantly reduce the computation in the optimal sizing of SWP systems.

To guarantee the validity of the proposed measurement method and implications, big data based wind power data analysis and SWP system simulations using a larger historical dataset from a more extensive geographic context are needed. The proposed method provides a promising new way to optimize the design of renewable energy systems.

References

[1] M.R. Patel, Wind and solar power systems: design, analysis, and operation, CRC press2005.

[2] J.K. Kaldellis, D. Zafirakis, The wind energy (r) evolution: A short review of a long history, Renewable energy 36(7) (2011) 1887-1901.

[3] I. Abouzahr, R. Ramakumar, Loss of power supply probability of stand-alone wind electric conversion systems: a closed form solution approach, IEEE Transactions on Energy Conversion 5(3) (1990) 445-452.

[4] L. He, S. Zhang, Y. Chen, L. Ren, J. Li, Techno-economic potential of a renewable energy-based microgrid system for a sustainable large-scale residential community in Beijing, China, Renewable and Sustainable Energy Reviews 93 (2018) 631-641.

[5] J.M. Lujano-Rojas, R. Dufo-López, J.L. Bernal-Agustín, Optimal sizing of small wind/battery systems considering the DC bus voltage stability effect on energy capture, wind speed variability, and load uncertainty, Applied Energy 93 (2012) 404-412.

[6] H. Li, P.E. Campana, Y. Tan, J. Yan, Feasibility study about using a stand-alone wind power driven heat pump for space heating, Applied energy 228 (2018) 1486-1498.

[7] B. Zhao, X. Zhang, P. Li, K. Wang, M. Xue, C. Wang, Optimal sizing, operating strategy and operational experience of a stand-alone microgrid on Dongfushan Island, Applied Energy 113 (2014) 1656-1666.

[8] M. Kapsali, J. Anagnostopoulos, J. Kaldellis, Wind powered pumped-hydro storage systems for remote islands: a complete sensitivity analysis based on economic perspectives, Applied energy 99 (2012) 430-444.

[9] A. Zerrahn, W.-P. Schill, Long-run power storage requirements for high shares of renewables: review and a new model, Renewable and Sustainable Energy Reviews 79 (2017) 1518-1534.

[10] M.B. Blarke, H. Lund, The effectiveness of storage and relocation options in renewable energy systems, Renewable Energy 33(7) (2008) 1499-1507.

[11] T. Ayodele, A. Ogunjuyigbe, Mitigation of wind power intermittency: Storage technology approach, Renewable and Sustainable Energy Reviews 44 (2015) 447-456.

[12] F. Díaz-González, A. Sumper, O. Gomis-Bellmunt, R. Villafáfila-Robles, A review of energy storage technologies for wind power applications, Renewable and sustainable energy reviews 16(4) (2012) 2154-2171.

[13] A. Berrada, K. Loudiyi, Operation, sizing, and economic evaluation of storage for solar and wind power plants, Renewable and sustainable energy Reviews 59 (2016) 1117-1129.

[14] M. Beaudin, H. Zareipour, A. Schellenberglabe, W. Rosehart, Energy storage for mitigating the variability of renewable electricity sources: An updated review, Energy for sustainable development 14(4) (2010) 302-314.

[15] H. Zhao, Q. Wu, S. Hu, H. Xu, C.N. Rasmussen, Review of energy storage system for wind power integration support, Applied energy 137 (2015) 545-553.

[16] P. Chen, T. Thiringer, Analysis of energy curtailment and capacity overinstallation to maximize wind turbine profit considering electricity price–wind correlation, IEEE Transactions on Sustainable Energy 8(4) (2017) 1406-1414.

[17] J. Kaldellis, E. Kondili, A. Filios, Sizing a hybrid wind-diesel stand-alone system on the basis of minimum long-term electricity production cost, Applied Energy 83(12) (2006) 1384-1403.

[18] A.S. Al Busaidi, H.A. Kazem, A.H. Al-Badi, M.F. Khan, A review of optimum sizing of hybrid PV–Wind renewable energy systems in oman, Renewable and Sustainable Energy Reviews 53 (2016) 185-193.

[19] M.D. Al-Falahi, S. Jayasinghe, H. Enshaei, A review on recent size optimization methodologies for standalone solar and wind hybrid renewable energy system, Energy Conversion and Management 143 (2017) 252-274.

[20] M. Albadi, E. El-Saadany, Overview of wind power intermittency impacts on power systems, Electric power systems research 80(6) (2010) 627-632.

[21] W. Katzenstein, J. Apt, The cost of wind power variability, Energy Policy 51 (2012) 233-243.

[22] B. Tarroja, F. Mueller, J.D. Eichman, J. Brouwer, S. Samuelsen, Spatial and temporal analysis of electric wind generation intermittency and dynamics, Renewable Energy 36(12) (2011) 3424-3432.

[23] W. Katzenstein, E. Fertig, J. Apt, The variability of interconnected wind plants, Energy policy 38(8) (2010) 4400-4410.

[24] G. Ren, J. Liu, J. Wan, Y. Guo, D. Yu, Overview of wind power intermittency: Impacts, measurements, and mitigation solutions, Applied Energy 204 (2017) 47-65.

[25] G. Ren, J. Liu, J. Wan, Y. Guo, D. Yu, J. Liu, Measurement and statistical analysis of wind speed intermittency, Energy 118 (2017) 632-643.

[26] J. Apt, The spectrum of power from wind turbines, Journal of Power Sources 169(2) (2007) 369-374.

[27] J. Jung, K.-S. Tam, A frequency domain approach to characterize and analyze wind speed patterns, Applied energy 103 (2013) 435-443.

[28] M.R.R. Tabar, M. Anvari, G. Lohmann, D. Heinemann, M. Wächter, P. Milan, E. Lorenz, J. Peinke, Kolmogorov spectrum of renewable wind and solar power fluctuations, The European Physical Journal Special Topics 223(12) (2014) 2637-2644.

[29] J.P. Fossati, A. Galarza, A. Martín-Villate, L. Fontan, A method for optimal sizing energy storage systems for microgrids, Renewable Energy 77 (2015) 539-549.

[30] C. Draxl, A. Clifton, B.-M. Hodge, J. McCaa, The wind integration national dataset (wind) toolkit, Applied Energy 151 (2015) 355-366.

[31] K. Zhou, J. Ferreira, S. De Haan, Optimal energy management strategy and system sizing method for stand-alone photovoltaic-hydrogen systems, International journal of hydrogen energy 33(2) (2008) 477-489.

[32] H. Yang, W. Zhou, L. Lu, Z. Fang, Optimal sizing method for stand-alone hybrid solar–wind system with LPSP technology by using genetic algorithm, Solar energy 82(4) (2008) 354-367.

[33] N. DiOrio, A. Dobos, S. Janzou, Economic analysis case studies of battery energy storage with SAM, National Renewable Energy Lab.(NREL), Golden, CO (United States), 2015.

[34] W. Kellogg, M. Nehrir, G. Venkataramanan, V. Gerez, Generation unit sizing and cost analysis for stand-alone wind, photovoltaic, and hybrid wind/PV systems, IEEE Transactions on energy conversion 13(1) (1998) 70-75.

[35] D. Nelson, M. Nehrir, C. Wang, Unit sizing and cost analysis of stand-alone hybrid wind/PV/fuel cell power generation systems, Renewable energy 31(10) (2006) 1641-1656